Collective phenomena in neuronal cultures recorded with MEAs

Author: Carmen Piñero Megías
*Facultat de Física, Universitat de Barcelona, Diagonal 645, 08028 Barcelona, Spain.**

Advisor: Jordi Soriano Fradera

Abstract: This study delves into the dynamics of living neuronal networks using a microelectrode arrays (MEAs) system. Through analysis of the neuronal activity of an *in vitro* neuronal network, we explored the short– and long–term effects of electrical stimulation on the network's functional connectivity, which was quantified through cross-correlation in combination with analyses from graph theory. Spatial coarse–sampling of the data revealed a complex relationship between electrode density and network properties, emphasizing the need to examine with care contradictory results in studies with MEAs. Our findings show the intricate interplay between stimulation, plasticity and resilience to damage in neuronal cultures.

I. INTRODUCTION

The study of neuronal cultures in the framework of complex systems and network science has become an active research field in recent years. One of the most interesting questions is *spontaneous activity*, i.e. the capacity of neurons to activate by themselves thanks to noise and fluctuations, and the rich relationship between spontaneous activity, network connectivity and plasticity [1]. The latter refers to the capacity of neurons to alter their connections to increase or decrease their activity, depending on information processing needs.

In this context, two main experimental approaches are employed to extract information about neuronal activity: calcium imaging and electrodes [2]. Calcium imaging uses fluorescent dyes to detect neuronal activity (action potentials or *spikes*), offering superior spatial resolution, with great detail of individual neuronal positions, but the time resolution is very poor, limited by the dye kinetics. Electrodes, by contrast, excel in time resolution, offering precise data associated to the electrical signals of neuronal spikes. However, electrodes are metallic and opaque, which impedes the detection of neuronal positions. Additionally, MEAs enable noninvasive extracellular recordings and localized electrical stimulation in the same setup, serving as a valuable tool for studying connectivity and its changes upon stimulation.

This project focuses on the analysis of data acquired from recordings of a cortical primary culture grown on an MEA system. The primary objective of this work is to serve as a proof of concept for the effects of stimulation on neuronal network dynamics. Through our analysis we aim to characterize the functional connectivity of the system upon different stimulation schemes, quantify the main properties of the network, and understand the changes it undergoes. We also aim to study how data sampling influences results and how this can be related to the electrode density of MEAs.

*Electronic address: cpinerme7@alumnes.ub.edu

II. MATERIALS AND METHODS

A. Multielectrode array chip

We analyzed data obtained from the recordings of a cortical rat primary culture grown on the MEA system, used in Dr. Soriano's Laboratory, from the Swiss company 3Brain. This system comprises a high–density microelectrode array (HD-MEA) chip featuring 4096 electrodes arranged in a 64×64 grid, covering an area of 3.84×3.84 mm^2 [Fig. 1(a)]. Each electrode measures 21×21 μm^2, therefore it can concurrently capture the signals of up to three neurons touching the electrode, in addition to weaker activity from neighbouring neurons.

The system allows to record spontaneous activity concurrently on its 4096 sites. For that, it has a resolution of 10 μA and a temporal resolution of 10 μs, which provides a high degree of precision in capturing neuronal events, which usually take place in the millisecond scale. This is a great advantage over calcium imaging recordings, which have a resolution of $10 - 20$ ms. The 3Brain system also enables electrical stimulation on any of the microelectrodes. The spikes of each electrode were extracted using the 3Brain software BrainWave 5 [Fig. 1(b)].

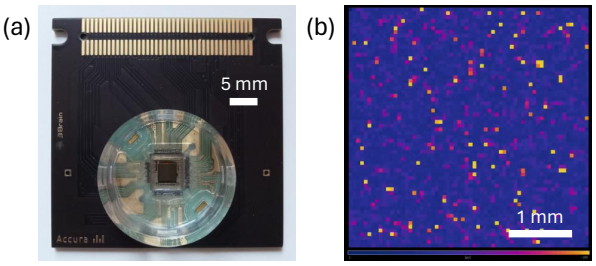

FIG. 1: 3Brain HD-MEA chip. (a) Picture of the chip and its electronics prior to using it to culture neurons, which are placed on the central squared area. The top pins are the interface with a computer. (b) A snapshot of neuronal activity in the chip, with 64×64 active sites, visualized with the BrainWave 5 software from 3Brain. Bright yellow spots are active electrodes.

B. Stimulation setup

The protocol used to obtain the electrodes' spikes data consisted of three main phases, termed 1, 2 and 3, as shown in Fig. 2(a). Each phase included a 5–minute recording of spontaneous activity. Phase 1 was also used to make a selection of the channels that had high activity. Stimulation was then applied on the selected channels, consisting of a fast train of 10 biphasic pulses, applied with a frequency of 20 Hz. Each electrical pulse had an amplitude of 5 μA, and a width of 100 μs. These trains were delivered every 10 s, 20 times in total (about 3.5 min).

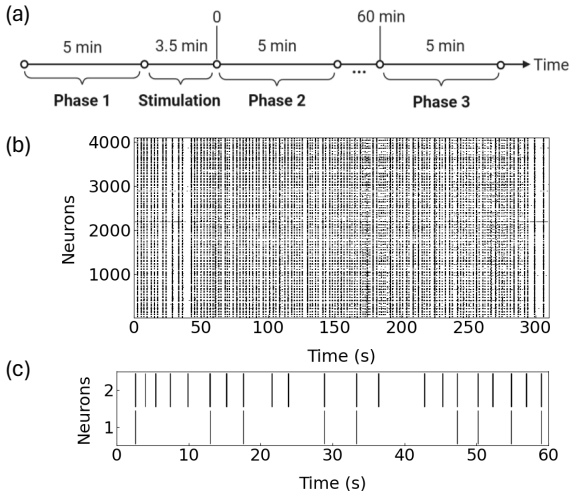

FIG. 2: Stimulation setup and data analysis. (a) Stimulation protocol used on neuronal cultures grown on the 3Brain MEA system. (b) Raster plot of spontaneous activity for phase 1 for all electrodes. (c) Representative trains of activity for phase 1 considering only 2 electrodes. Here, bars represent neuronal spikes in a time window of 0.01 s. Each pair of trains is used to compute the pairwise correlation matrix.

C. Data analysis

For clarity, sometimes we will use 'neuron' when describing the results, although all data comes from electrodes that may contain the signal of multiple neurons.

Data processing involved first the extraction of spikes. In either phase, a *raster plot* of activity was created, as depicted in Fig. 2(b). This plot represents the detected spikes, i.e., the activity of the culture.

To study the connectivity of the system, we applied the following method: a 'train' was assigned to each neuron, which consisted of an array comprising binary values (0 or 1), denoting whether the neuron had fired (1) or not (0) within a time window of 0.01 s [Fig. 2(c)]. This value was selected to align with the maximum time resolution of the MEA system. The pairwise correlation matrix was then computed. This matrix provides insights into the interdependencies between pairs of electrodes, allowing us to study *functional* connectivity of the network [3]. Each element r_{xy} of the matrix was computed as

$$r_{xy} = \frac{\sum(x_i - \bar{x})(y_i - \bar{y})}{\sqrt{\sum(x_i - \bar{x})^2 \sum(y_i - \bar{y})^2}}, \tag{1}$$

where x_i represents each value of the train corresponding to electrode x and $\bar{x}$ is the average of all the train values of electrode x. Similarly, y_i and $\bar{y}$ refer to the values and average of the train corresponding to electrode y, respectively. The summation goes over all the values of the train. If two neurons frequently spike in the same time window, as pictured in Fig. 2(c), they are considered strongly correlated and the matrix element $r_{xy} \simeq 1$. This indicates a strong functional connection between the two neurons.

The pairwise correlation matrix was binarized using a threshold of 0.4, i.e., all entries $r_{xy} < 0.4$ were set to 0, and otherwise to 1, shaping a connectivity matrix A_{xy}. This was done to remove noise–related activity and maintain only the strongest connections. Subsequently, the next network measures were computed:

• *Average connectivity* $\langle k \rangle$. It was computed as the total number of connections over the total number of electrodes N, i.e., $\langle k \rangle = \sum_{x,y} A_{xy}/N$.

• *Global efficiency* G_E. It varies between 0 and 1 and informs about the easiness of information propagation across the whole network [4]. The higher the density of connections in the network, the easier it is for the system to globally communicate and the higher G_E. It was calculated through the function `efficiency_wei()`, which uses Dijkstra's algorithm to calculate the shortest path length $d(x, y)$ between all possible pairs of nodes. Then, G_E is given by:

$$G_E = \frac{1}{N(N-1)} \sum_{1 \le x,y \le N} \frac{1}{d(x,y)}. \tag{2}$$

• *Modularity* Q. It varies between 0 and 1 and depicts the presence of modules or communities in the network. Communities are formed by nodes that are more densely connected between each other than with the rest of the network. High Q values imply stronger community structure [5]. The identification of communities within the network was achieved through the Matlab function `community_louvain()`, which employs a recursive algorithm to assign neurons onto modules. For clarity of visualization, the matrix A of functional connections was reordered to highlight communities along the diagonal.

In addition to the functional analysis, we performed a spatial coarse–sampling of the data, conceptually representing how data would be if, instead of 4096 electrodes, we would have had 1/4 of them, and so on. A script in Python was used to sample the data from each time window in the neuron trains into grids of varying sizes $n \times n$, where $n = 2, 4, 8$ and 16, leading to a down–sampling of the system to 1024, 256, 64 and 16 total electrodes, respectively. For each sample, a centre of the grid was

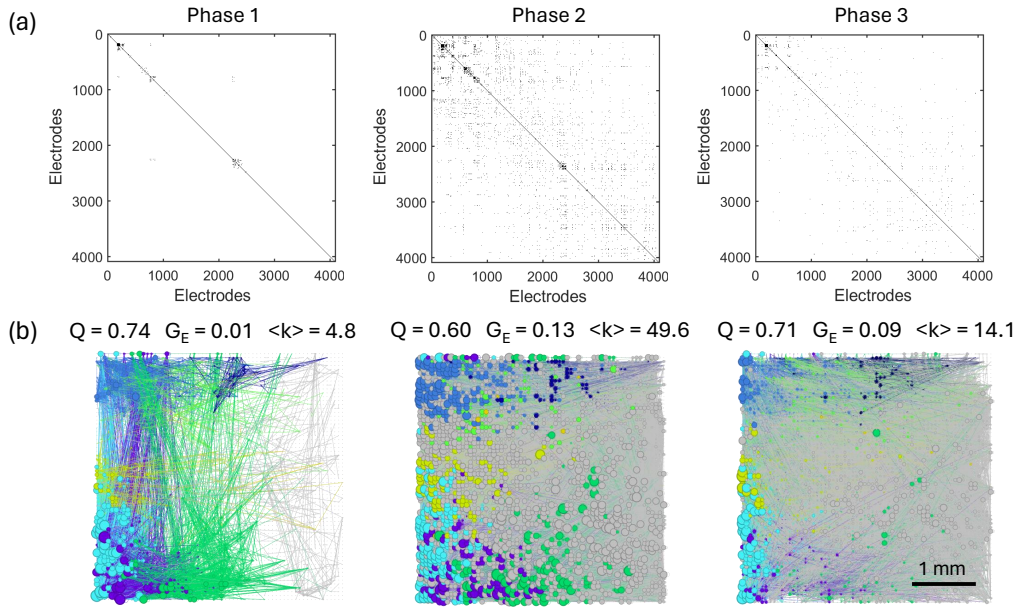

FIG. 3: Culture's connectivity for each phase of the experiment. (a) Connectivity matrices for phases 1, 2 and 3 respectively. (b) Graph representation of connectivity for the same phases. Circular objects are active electrodes, and their diameter is proportional to their connectivity. The different colors indicate the communities where the electrodes belong to.

designated, and the spikes of neighbouring points (which are 0 or 1) were weighted according to their distance to the centre, resulting in the new value. This process was systematically applied to all time windows. Finally, the whole analysis package was repeated to obtain the corresponding connectivity matrices and network descriptors.

III. RESULTS AND DISCUSSION

A. Functional connectivity

Once the connectivity matrices of each experiment phase are obtained, we can compare them. Fig. 3 shows the differences in the system before (phase 1) and after (phase 2) stimulation. We observed that, immediately following stimulation, the connectivity of the network substantially increases, as appreciated both visually (higher density of points in the matrix of phase 2) and in the average connectivity $\langle k \rangle$. New connections emerge and the whole system is visibly richer, i.e., the network has become much more integrated, as indicated by the decrease in modularity Q. Global efficiency G_E increases too after stimulation, indicating that the flow of information across the network is potentiated.

One hour after stimulation, in phase 3, the system has notably reduced its connections, tending towards its pre-stimulation state. However, some connections established during phase 2 persist, evident in both connectivity matrices and graphs, as seen in Fig. 3(a) and 3(b), respectively. Both G_E and $\langle k \rangle$ decrease, yet they do not fully return to their original values at phase 1. A similar behaviour is observed in Q. This evidences the presence of plasticity mechanisms but also some kind of resilience against modifications in the network.

If we look at the graphs, we see that the main communities of the network are maintained throughout the different experimental phases. This also demonstrates a certain degree of robustness of the system against immediate modifications. On the other hand, communities also undergo alterations and some of them become more important after stimulation (grey and yellow communities in phases 2 and 3), while others reduce their size (purple and green communities in phase 3).

The observed persistence of altered connections post-stimulation implies enduring changes in the network's functional organization, emphasizing the lasting impact of the applied stimulation on the system. This dynamic shift suggests a manifestation of homeostatic plasticity mechanisms, such as synaptic scaling, wherein the strength of excitatory synapses is adjusted to compensate for activity variations, driving functional reorganization and contributing to network–wide resilience. Indeed, in the literature, recovered neuronal networks after chemical–induced damage [6] show a decrease in the density of effective links, accompanied by an increase in the average weights of retained links. This points to a rerouting of information flow along fewer, yet stronger, paths, as reflected in the G_E in our system.

B. Coarse–sampling effects

We performed a coarse–sampling of the obtained data [Fig. 4(a)] to evaluate if the system maintained its properties. We calculated the connectivity matrices, graphs

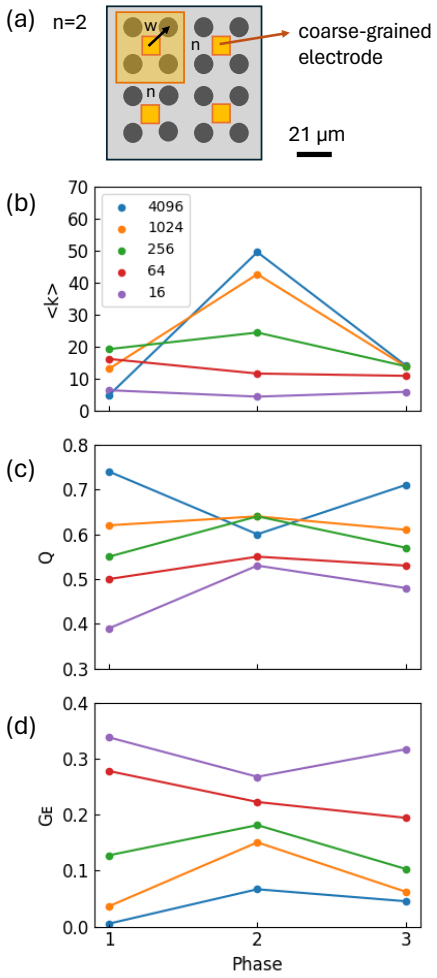

FIG. 4: Impact of coarse–sampling. (a) Sketch of the coarse–sampling operation for $n = 2$. (b)–(d) Evolution of the network parameters over the experimental phases for different coarse–sampling sizes.

and the main descriptors of the network for each phase and each coarse–sampling size. The results for Q, G_E and $\langle k \rangle$, as shown in Fig. 4(b)-(d).

We can observe that the modularity Q changes substantially with the sampling size. For the original network, we observed a significant decline of Q in phase 2, which was expected because the system is more integrated and overall connected. This pattern is broken when we examine the coarse–sampling results: Q increases right after stimulation for all sizes. Additionally, the initial and average values of Q throughout the different phases decrease when sampling size increases. This is expected because it is a consequence of this type of sampling: correlation increases, resulting in a more connected system, which is translated into a lower Q value.

Regarding average connectivity $\langle k \rangle$, an intriguing effect emerges. In the first phase, no correlation with sampling size is observable. However, in the second phase, larger sizes (lower total number of electrodes) correlate with lower $\langle k \rangle$ values. This may initially seem surprising given that we have seen the system becomes more integrated after coarse–sampling, but, if we study the $\langle k \rangle$ relative to the system size, we see that there is a rise with size: each neuron is connected to a higher fraction of total neurons. This manifests what we have previously mentioned, namely that overall connectivity is increased with coarse–sampling size.

While most cases show an increase in $\langle k \rangle$ after stimulation, for 64 and 16 total electrodes, it actually decreases and the difference between phases is much more subtle. This discrepancy suggests that the sample size is too small in these cases, resulting in a loss of richness of the system and implying the existence of a limit for the maximum sampling size before losing critical information.

Fig. 4(c) illustrates that global efficiency is lower in all three phases for the original size, and it increases with size, which is consistent with the idea that coarse–sampling shapes a more integrated system.

We observed in the literature that the choice of sampling technique to obtain neuronal data significantly influences the collective properties of the system. Temporal binning, thresholding and measurement overlap due to electrode proximity introduce various types of bias, adding correlations to the data. For the same parameters and dynamic state, coarse–sampling generates larger correlations than sub–sampling [7].

In our study we found big fluctuations depending on size and the general behaviour between phases is not consistently maintained. This interdependence between coarse–sampling size and the resulting network parameters suggests that network characterisation is intricately linked to the density of electrodes in the MEA system, which could indicate that the actual underlying dynamics are being overshadowed.

We can compare the connectivity matrices and graphs generated for different coarse–sampling sizes with the original ones, for phase 2 of the experiment, as depicted in Fig. 5. We observe that the main communities persist across the various sampling sizes, and they become more apparent when the grid size is increased, which corresponds to a lower number of total electrodes (see $n = 256$ in Fig. 5(a)). As a consequence of the sampling, a substantial number of total connections are lost. However, in the graphs, the colours representing the main communities are maintained. Some communities are more important when size is increased and they expand, as observed in the yellow and blue communities of Fig. 5(b). Nevertheless, there is a noticeable preservation of the overall community distribution in the network.

These results suggest that even less dense MEAs could serve for community identification effectively, however, they may not be convenient for the characterisation of the network's properties, as demonstrated in our analysis.

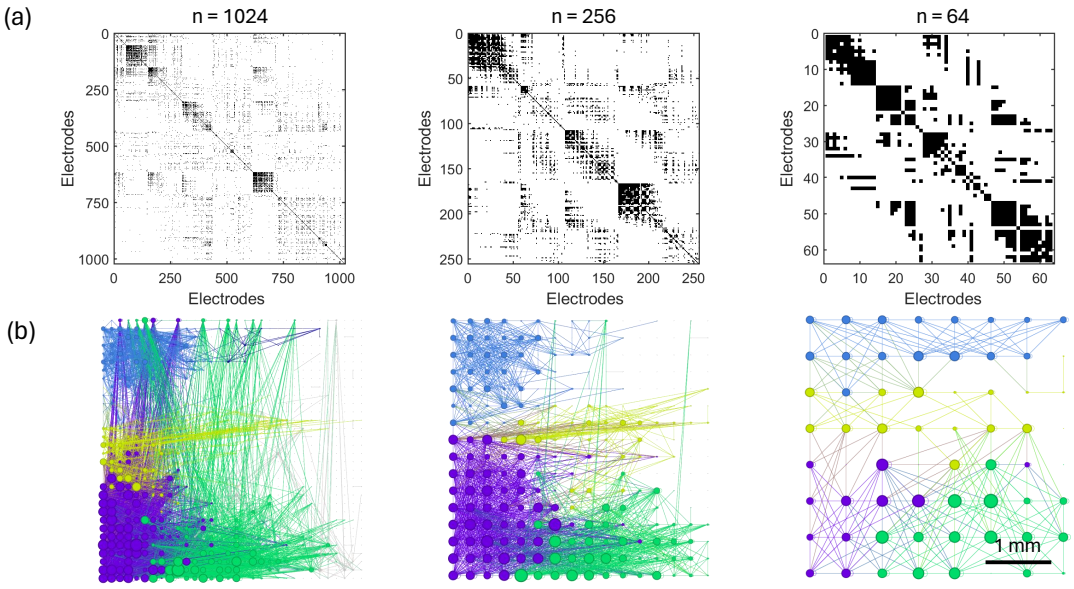

FIG. 5: Network connectivity in phase 2 of the experiment for each coarse–sampling size: 1024, 256 and 64 total electrodes respectively. (a) Connectivity matrix for each size. (b) Corresponding graphs. Circular objects are active electrodes, and their diameter is proportional to their connectivity. The different colours indicate the communities where the electrodes belong to.

IV. CONCLUSIONS

Our investigation into collective phenomena in neuronal cultures, especially focused on functional connectivity, has obtained insightful observations of the effects of stimulation on the dynamics of neuronal networks.

By examining post–stimulation phases, we observed enduring changes in the functional organization of the network. This persistence of altered connections as well as a certain resilience against perturbations highlights the impact of applied electrical stimulation and suggests the manifestation of homeostatic plasticity mechanisms. It has already been shown that stimulation enables training and feedback responses of neuronal cultures, which opens new avenues to the possibility of developing treatments for certain neurological diseases or even artificial intelligence capabilities in *in vitro* systems.

Our coarse–sampling analysis provided further insights, emphasizing the interplay between electrode density and network properties. The fluctuating values of network descriptors across different sampling sizes underscore the sensitivity of network characterization to the spatial arrangement of electrodes in MEA systems. Notably, the maintenance of main communities across various sampling sizes suggests that, while electrode density influences collective properties, it might not be as decisive for community identification.

Our results, while offering contributions to the understanding of neuronal network dynamics, also emphasize the need for caution when comparing data across studies that utilize MEAs of different electrode densities. Further studies are crucial for ensuring the reliability and reproducibility of findings in MEA–based studies.

Acknowledgments

I would like to express my sincere gratitude to my supervisor Dr. Jordi Soriano for his excellent guidance and expertise. I am also grateful to Akke Mats Houben and Anna-Christina Haeb for their assistance and support.

[1] J. Orlandi et al. “Noise focusing and the emergence of coherent activity in neuronal cultures”. Nature Phys **9**, 582–590 (2013).
[2] Z. Wei et al. “A comparison of neuronal population dynamics measured with calcium imaging and electrophysiology”. PLOS Comput. Biol. **16**, e1008198 (2020).
[3] G. Zamora-López et al. “Functional complexity emerging from anatomical constraints in the brain”. Sci Rep **6**, article 38424 (2016).
[4] J. Soriano. “Neuronal Cultures: Exploring Biophysics, Complex Systems, and Medicine in a Dish”. Biophysica **3**, 181-20 (2023).
[5] M.E. Newman, “Modularity and community structure in networks”. PNAS **23**, 8577–8582 (2006).
[6] E. Estévez-Priego et al. “Functional strengthening through synaptic scaling upon connectivity disruption in neuronal cultures”. Net. Neurosci. **4**, 1160–1180 (2020).
[7] J. P. Neto et al. “Sampling effects and measurement overlap can bias the inference of neuronal avalanches”. PLOS Comput. Biol. **18**, e1010678 (2022).